

# NMR Based Methods for Metabolites Analysis

Published as part of *Analytical Chemistry special issue "Fundamental and Applied Reviews in Analytical Chemistry 2025"*.

Lichun He,<sup>#</sup> Bin Jiang,<sup>#</sup> Yun Peng, Xu Zhang, and Maili Liu\*



Cite This: *Anal. Chem.* 2025, 97, 5393–5406



Read Online

ACCESS |

Metrics & More

Article Recommendations

**ABSTRACT:** Metabolite analysis is essential for understanding the biochemical processes and pathways that sustain life, providing insights into the complex interactions within cellular systems and clinical examinations. This review explores recent applications of nuclear magnetic resonance (NMR) spectroscopy in metabolite studies. Various methods enhancing analytical accuracy for metabolome profiling and metabolic pathway studies, including spectral simplification techniques, quantitative NMR, high-resolution MAS NMR, and isotopic labeling, are discussed. The application of NMR in *in situ* and *in vivo* studies is also covered, highlighting in-cell NMR and *in vivo* MRS techniques. Last but not least, we discuss recent advancements in NMR hyperpolarization, with a focus on dynamic nuclear polarization (DNP), chemically induced dynamic nuclear polarization (CIDNP), para-hydrogen-induced polarization (PHIP), and signal amplification by reversible exchange (SABRE). These advancements offer significant potential for enhancing the sensitivity and accuracy of metabolite studies and are expected to further deepen the study and understanding of metabolites and metabolic pathways.

## ■ INTRODUCTION

Metabolites are small molecules that serve as intermediates or end products of metabolism within biological systems, playing essential roles in various biochemical processes, such as energy production,<sup>1–3</sup> signal transduction,<sup>4–6</sup> and the synthesis of cellular components.<sup>7–9</sup> The discovery, identification, and analysis of metabolites are fundamental to understanding metabolic pathways and regulation mechanisms. Spectroscopy is a widely employed analytical technique in metabolite studies, enabling the identification, characterization, and quantification of these small molecules. Among the available methods, mass spectroscopy (MS) and nuclear magnetic resonance (NMR) spectroscopy are the two most commonly employed techniques, each with distinct advantages. MS offers high sensitivity and can detect analytes at concentrations ranging from low picomolar to femtomolar levels. However, it is inherently destructive to samples and frequently requires derivatization or complex extraction steps prior to analysis. On the other hand, NMR allows for repeated measurements with accurate quantification, supporting real-time monitoring of metabolites changes, and is invaluable for characterizing complex metabolite mixtures and profiling metabolic changes. Additionally, NMR can be adapted for live-cell and tissue studies as well as on-site analysis. Other spectroscopic methods, such as infrared (IR) and UV–vis spectroscopy, are less commonly used in the study of metabolites.

In this review, we focused on the current applications of NMR spectroscopy in metabolite studies. We first introduced spectral simplification techniques, such as singlet state filtering and pure shift methods, which enhanced the resolution and clarity of NMR spectra. Following this, we highlighted the

strengths of NMR spectroscopy in the identification and quantification of small molecule and peptide metabolites, emphasizing its accuracy and reliability. We also explored the integration of NMR with computational methods and the generation of comprehensive databases, enhancing the metabolite identification and analysis. Additionally, we discussed the study of metabolomic profiling and the elucidation of metabolic pathways, extending the application of NMR to in-cell and *in vivo* studies of metabolites and metabolic pathways in their native biological environments. Lastly, we reviewed the innovative application of NMR hyperpolarization techniques, which significantly enhance signal sensitivity and enable the detection of low-abundance metabolites.

## ■ SPECTRAL SIMPLIFICATION USING SINGLET STATE FILTERING OR PURE SHIFT TECHNIQUES

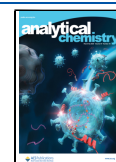
One challenge faced by <sup>1</sup>H NMR is that when the sample composition is complex, severe peak overlapping occurs due to the narrow range of chemical shift distribution of <sup>1</sup>H nuclei and J coupling splitting. This hinders the resolution of the spectral peaks and the extraction of information. Besides traditional multidimensional NMR methods, recent years have seen the emergence of techniques such as singlet state

**Received:** November 30, 2024

**Revised:** February 7, 2025

**Accepted:** February 19, 2025

**Published:** March 6, 2025



filtering<sup>10,11</sup> and pure shift techniques<sup>12</sup> for spectral simplification.

**Singlet State Filtering.** A spin system composed of a pair of coupled spin-1/2 particles has a total spin quantum number of either 0 or 1. The spin-0 state is known as the singlet state, while the spin-1 state includes three components and is termed the triplet states. When two spin-1/2 nuclei are magnetically equivalent, the energy eigenstates of this double spin system are the singlet state and the triplet state, and transitions between them are slow. This results in the singlet state having a much longer lifetime than the T<sub>1</sub> relaxation time of the nuclear spin.<sup>13</sup> The long-lived singlet state can be converted into normal NMR coherence to observe in a magnetically inequivalent environment; therefore, it can be used to study slow molecular processes and also for the storage of hyperpolarized nuclear spins.

The first pulse sequence used for singlet state filtering<sup>11</sup> was general coupling M2S (gc-M2S), but this pulse sequence utilized many 180-degree hard pulses, which may lead to sample heating. Moreover, the sequence does not perform well on weakly coupled multispin systems. Huang et al. applied adiabatic passage singlet order conversion (APSOC) method to singlet state filtering experiments, avoiding the risk of sample heating and making it suitable for both strongly and weakly coupled systems.<sup>14</sup> The author applied the singlet state filtering method to a grape sarcocarp sample, suppressing the strong water peak and other background signals and only displaying the selected coupled <sup>1</sup>H spin system in the spectrum.

*In vivo* NMR can noninvasively detect metabolites within living organisms and is significantly important in fields such as biology and medicine. However, there is usually severe peak overlapping in *in vivo* NMR, and spectral broadening caused by magnetic field inhomogeneity further reduces the resolution of *in vivo* NMR, posing challenges for precise monitoring and analysis of metabolic changes within organisms. By injecting or feeding test subjects with <sup>13</sup>C-labeled metabolites, it is possible to use <sup>13</sup>C NMR to eliminate the influence of background signals and obtain *in vivo* information on metabolic processes. However, this method is expensive, especially when used for long-term metabolic studies. In comparison, singlet-filter based <sup>1</sup>H NMR<sup>11</sup> offers a more cost-effective advantage. Glutamate (Glu) and glutamine (Gln) are two important amino acids that play crucial roles in biological organisms. Detecting Glu and Gln *in vivo* is of significant importance for neuroscience and medicine. Xin et al. utilized optimized control methods to specifically optimize the M2S (Magnetization to Singlet) and S2M (Singlet to Magnetization) pulses used in singlet NMR experiments.<sup>15</sup> This enhanced the efficiency of converting magnetization into the singlet state in the <sup>1</sup>H nuclear spin systems of Glu and Gln, successfully achieving the selective *in vivo* detection of Glu and Gln. Another example of singlet filter technology used in *in vivo* NMR is by Lysak et al., who applied it to study the metabolic changes in *Daphnia magna*, an aquatic keystone species and model organism, in response to anoxic stress.<sup>16</sup>

**Pure Shift Techniques.** Compared with <sup>1</sup>H NMR spectra, the <sup>13</sup>C NMR spectra of <sup>13</sup>C nucleic natural abundance samples have a distinct advantage. By application of composite pulse irradiation to <sup>1</sup>H nuclei during sampling, broadband decoupling of <sup>1</sup>H nuclei in the <sup>13</sup>C spectra is achieved. This eliminates the <sup>1</sup>H–<sup>13</sup>C J-coupling splitting, thereby significantly enhancing the resolution of the <sup>13</sup>C spectra. This

encourages the continuous development of homonuclear broadband decoupling techniques in <sup>1</sup>H NMR, also known as pure shift techniques.<sup>12</sup> Pure shift techniques include bilinear rotational decoupling (BIRD),<sup>17</sup> slice-selective (Zangger–Sterk) decoupling,<sup>18</sup> and PSYCHE decoupling,<sup>19</sup> with the latter considered to be the best pure shift technique available to date.

Along with singlet state filtering, pure shift techniques can also undoubtedly enhance the resolution of spectra by eliminating J-coupling splitting. However, the intensity and shape of signals in pure shift spectra are influenced by experimental parameters of the pure shift technique as well as factors such as chemical shifts and J-coupling in the nuclear spin system. This poses challenges for using pure shift spectra in quantitative metabolomics research. Chen et al. collected pure shift spectra of some metabolites of interest at various concentrations using the same pure shift experimental parameters. These pure shift spectra can be used as reference spectra to quantitatively measure these metabolites of interest in biological samples using pure shift techniques.<sup>20</sup>

When using NMR for component analysis of mixtures, the conventional method is diffusion ordered spectroscopy (DOSY). However, when the diffusion coefficients of the components are similar, the DOSY struggles to differentiate between components. In 2017, GA Morris's research group introduced the REST (Relaxation Encoded Selective TOCSY) method,<sup>21</sup> where selective TOCSY techniques were applied to ensure that all signals within a spin system receive the same relaxation weighting, thereby utilizing differences in relaxation time constants for component discrimination. However, the application of REST encounters difficulties when there is spectral peak overlap. Smith et al. combined pure shift techniques with the REST pulse sequence, leveraging the resolution improvement brought by pure shift to avoid many cases of peak overlap, thus expanding the scope of using relaxation differences for mixture component analysis.<sup>22</sup>

Pure shift techniques enhance spectral resolution through broadband homonuclear decoupling, but it loses the information on J-coupling, which contains valuable data on structural bonding and coupling networks helpful for molecular structural determination. Zhan et al. combined pure shift technique with 2D J-based DOSY to propose the in-phase pure shift J-DOSY sequence method.<sup>23</sup> This approach produces a 3D spectrum of the sample, featuring one dimension of broadband homonuclear decoupled chemical shifts, one dimension of J-coupling, and one dimension of diffusion coefficients. This technique reduces peak overlap in DOSY using the pure shift technique while retaining J-coupling information.

## ■ IDENTIFICATION AND QUANTIFICATION OF METABOLITES

### NMR Identification of Small Molecule Metabolites.

Most metabolites are low-molecular-weight organic compounds, such as lactic acid, glutamate, and cholesterol.<sup>24,25</sup> Various NMR techniques provide valuable information for the identification and tracking of small molecule metabolites. One-dimensional (1D) NMR, especially <sup>1</sup>H NMR, is frequently employed for confirming organic compounds due to its ease of use and straightforward sample preparation, which typically involves simply dissolving the analyte in a deuterated solvent. The simplicity of the 1D NMR setup and automated instrument configuration also makes it accessible

for those new to NMR spectroscopy. 1D NMR, particularly  $^1\text{H}$  NMR, offers good sensitivity, contributed by its natural abundance of isotopes, making it suitable for detecting low concentrations of small molecules. 1D NMR experiments generally require short acquisition times, ranging from minutes to a few hours, enabling rapid data collection. Interpretation of 1D NMR spectra is relatively straightforward, as the signals correspond directly to specific nuclei, facilitating structural information and relative quantification of metabolites. Overall, 1D NMRs is a quick and reliable method for tracking metabolites.

In clinical application, 1D  $^1\text{H}$  NMR or magnetic resonance spectroscopy (MRS) is used to detect and measure cellular metabolites, aiding in the early diagnosis of diseases.<sup>26,27</sup> For example, Ana Gil and co-workers identified and evaluated metabolites in saliva using  $^1\text{H}$  NMR in 2020.<sup>28</sup> Employing 1D  $^1\text{H}$  NMR, they successfully identified various metabolites in the saliva of standard healthy adults under different conditions after collection (Figure 1). Through the identification of 22

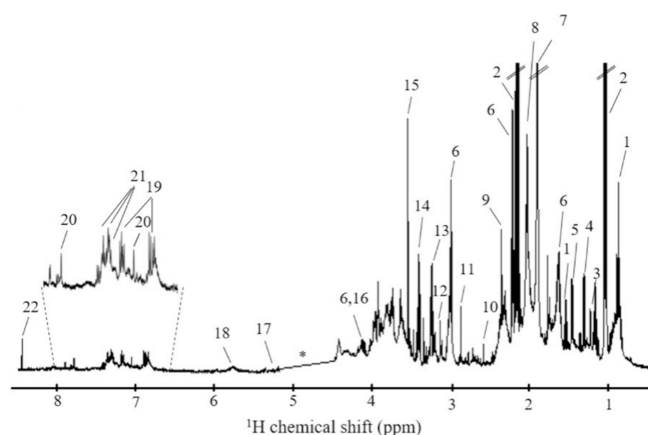


**Figure 1.**  $^1\text{H}$  NMR spectra of saliva of a healthy female adult collected and analyzed in the study. Multiple metabolites were assigned: 1, butyrate; 2, propionate; 3, fucose; 4, lactate; 5, alanine; 6, 5-aminopentanoate; 7, acetate; 8, N-acetyl (glycoproteins); 9, pyruvate; 10, methylamine; 11, trimethylamine; 12 dimethyl sulfone; 13, betaine; 14, taurine; 15, glycine; 16, proline; 17, xylose; 18, urea; 19, tyrosine; 20, histidine; 21, phenylalanine; 22, formate. Reproduced from Duarte, D.; Castro, B.; Pereira, J. L.; Marques, J. F.; Costa, A. L.; Gil, A. M. Evaluation of saliva stability for NMR metabolomics: collection and handling protocols. *Metabolites* 2020, 10(12), 515 (ref 28). Copyright 2020 MDPIbooks.

distinct metabolites, they observed significant interindividual and interday metabolic variability, which likely reflects sample stability to some extent in the context of clinical examinations. Notably, metabolites such as galactose and hypoxanthine were identified as potential stability indicators for saliva samples, underscoring their relevance in ensuring the sample quality for NMR-based metabolomics analyses.

2D NMR methods provide detailed insights into molecular structure, dynamics, and interactions. For example, the widely used correlation spectroscopy (COSY) technique identifies spin–spin coupling between directly bonded protons, establishing connectivity within a molecule and creating a visual correlation map of coupled protons that aids in deducing organic compound structures. Heteronuclear multiple bond correlation (HMBC) detects long-range correlations between protons and carbons, which are particularly useful for

confirming functional groups and determining more complex or larger molecular structures. Nuclear Overhauser effect spectroscopy (NOESY) is valuable for studying molecular interactions such as ligand–receptor binding and conformational changes in metabolites. Eugene Kwan and Shaw Huang highlighted the strengths and unique aspects of various 2D NMR techniques for organic molecule structure in a minireview.<sup>29</sup> They presented an example analysis of methanol, a metabolite involved in the metabolism of certain fruits and vegetables. They initially identified an aliphatic alcohol functional group using 1D  $^1\text{H}$  NMR. Starting with the methyl groups, they identified a diastereotopic isopropyl fragment through the COSY and HMBC correlations. Further COSY analysis revealed other CH groups, and by examining chemical shifts, they assigned the CH group adjacent to the OH functional group (Figure 2). Finally, they confirmed con-

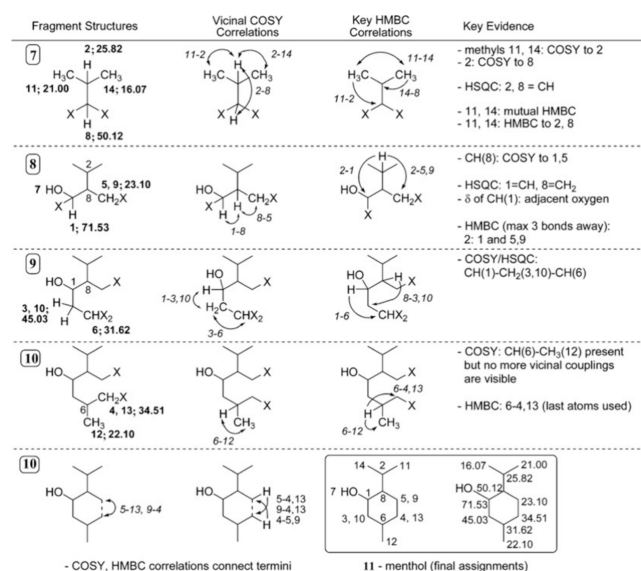


**Figure 2.** Step-wise structural elucidation of methanol using COSY and HMBC 2D NMRs. Reproduced from Structural elucidation with NMR spectroscopy: practical strategies for organic chemists, Kwan, E. E.; Huang, S. G. *Eur. J. Org. Chem.*, Vol. 2008, Issue 16 (ref 29). Copyright 2008 Wiley.

nectivity with HMBC correlations, arriving at the correct structure of the methanol. Overall, 2D NMR, in combination with 1D methods, provides a nuanced and comprehensive view of small molecule metabolites, facilitating detailed structural elucidation and enhanced understanding of molecular behavior.

**NMR Identification of Peptides Metabolites.** Some peptides are also considered metabolites as they are produced through metabolic processes and serve various biological roles. For example, peptide hormones like insulin and glucagon are key metabolites involved in glucose metabolism,<sup>30,31</sup> neuro-peptide like substance P and endorphins play roles in neurotransmission that influence pain perception and mood,<sup>32,33</sup> and antimicrobial peptides like defensins and cathelicidins are components of the immune response.<sup>34,35</sup> Although these metabolites are oligopeptides that are generally smaller than proteins, consisting of 5 to 50 amino acid residues. The larger and more complex structures, compared to small molecule metabolites, lead to more crowded 1D spectra. As a result, 2D NMR techniques are more commonly



employed to study peptide metabolites. Additionally, more complex NMR experiments, including 3D or anisotropic methods, are sometimes used to resolve peptide metabolites.

Molecular structure and physiological properties of insulin was studied via 1D  $^1\text{H}$  NMR for decades.<sup>36,37</sup> Earlier this year, Tommy Wong et al. explored metabolic profiling of various glycemic traits.<sup>38</sup> Using high-throughput NMR and 1D  $^1\text{H}$  NMR, they established genetic associations with several biomarkers, including monomeric insulin, as well as associations between fast insulin and other circulating metabolites. More complex NMR methods are employed in mechanistic studies of insulin equilibrium and homeostasis. It is known that insulin predominantly exist in hexameric form in bloodstream and dissociate into monomeric form to exert biological effects.<sup>39,40</sup> Lech Kozerski and co-workers investigated insulin oligomer diffusion coefficient and the impact of pH on the insulin aggregation using a 3D  $^{13}\text{C}/^{15}\text{N}$ -HSQC-iDOSY NMR experiment.<sup>41</sup> This experiment, conducted on fully  $^{13}\text{C}$ ,  $^{15}\text{N}$ -labeled insulin, produced diffusion-ordered HSQC spectra, enabling the assignment of individual diffusion coefficients.

Like insulin, glucagon plays a role in maintaining blood glucose homeostasis. Glucagon is insoluble at neutral pH, soluble but prone to chemical degradation at basic pH,<sup>42</sup> and stably soluble at acidic pH though its fibrillization within hours.<sup>43</sup> Yongchao Su, Mei Hong, and co-workers investigated the formation and structure of glucagon amyloid fibrils using 2D solid-state NMR in 2019.<sup>44</sup> They analyzed 2D  $^{13}\text{C}$ – $^{13}\text{C}$  correlation and  $^{15}\text{N}$ – $^{13}\text{C}\alpha$  correlation spectra, assigning all amino acid residues and distinguishing two distinct conformers. Coupled with microscopy, their finding showed that glucagon self-assembled into fibril as a rigid  $\beta$ -strand, extending to approximately 10 nm, and forming antiparallel hydrogen-bonded  $\beta$ -sheets.

### Computational Assisted Analysis of Metabolites.

Various NMR methods have been extensively used for metabolite identification, providing robust fingerprints for hundreds of metabolites in biological samples. To simplify the manual process and enhance the accuracy of structural elucidation, large databases and a machine learning framework have become increasingly essential. David Wishart and his team established the Human Metabolome Database (HMDB), offering comprehensive, high-quality data on human metabolites, including their biological, physiological, and chemical properties.<sup>45</sup> The current version HMDB 5.0, updated in 2022, contains data on 217 920 metabolites, with detailed descriptions, identification information, chemical taxonomy, ontology, physical properties, experimental and predicted mass spectroscopy (MS) and NMR spectra, biological properties, diagnostic standards, referenced articles, and metabolite associated proteins. This database is a valuable resource for metabolite identification, metabolite research, and related clinical applications.

Using the HMDB and other databases, Matthew Kanan and co-workers reported their work on a machine learning framework for automated structure elucidation from 1D NMR spectra in 2021.<sup>46</sup> The input data included a full  $^1\text{H}$  NMR spectrum,  $^{13}\text{C}$  NMR peaks, and the molecular formula, which were passed through a neural network trained to identify substructures. The output was a substructure probability profile, indicating the likelihood of each substructure being present. The resulting molecular structures were generated using a graph generation algorithm, which takes the molecular formula and substructure probability profile as inputs, with the

structure corresponding to the lowest score being the most probable (Figure 3).

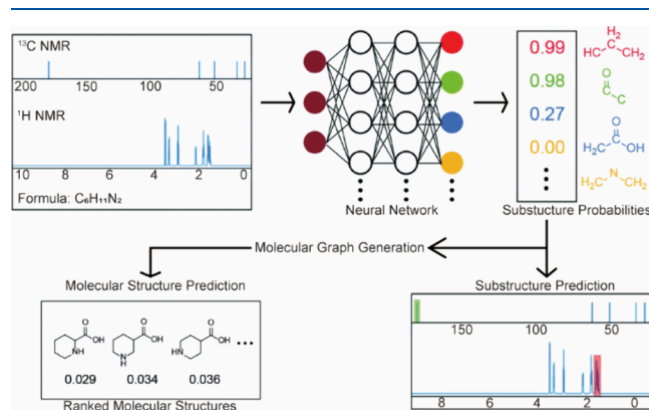


**Figure 3.** Overview of the automated structure prediction framework, demonstrated with the proline example. Reproduced from Huang, Z.; Chen, M. S.; Woroch, C. P.; Markland, T. E.; Kanan, M. W. *Chem. Sci.* 2021, 12, 15329 (ref 46), with permission of The Royal Society of Chemistry.

Isabel Garcia-Perez et al. summarized a protocol for metabolite identification using NMR spectroscopy in 2020,<sup>47</sup> which included sample preparation, data acquisition, and the data modeling. Computational modeling played a key role after NMR spectra were obtained, incorporating techniques such as database matching and spiking, following 2D NMR correlation measurements. Other methods included correlation modeling to reduce unrelated NMR signals in the data set and automated matching of correlated chemical shift peaks with spectral databases.

Xiongjie Xiao et al. reported their research on development of a Restore High-resolution Unet (RH-Unet) postprocessing method for correcting distorted NMR spectra acquired in inhomogeneous magnetic fields using a convolutional neural network in 2023.<sup>48</sup> The RH-Unet model was trained to map low-resolution spectra to high-resolution ones and demonstrated superior performance compared to the deconvolution method incorporated in the Bruker Topspin software. This approach enabled the acquisition of high-resolution NMR spectra under inhomogeneous field conditions, broadening its potential applications across various fields.

The combination of computational methods, such as database integration and matching, machine learning and neural network, and molecular and spectra modeling, can significantly enhance the study of metabolites, particularly for compound identification and structural analysis. Furthermore, the hybrid approach can be transformative for metabolomics studies and organic chemistry researches.

## METHODS FOR STUDY OF METABOLOME PROFILING AND METABOLIC PATHWAYS

The metabolome refers to the set of metabolites present in a biological system at a given time under specific conditions. Monitoring changes in the presence and concentration of metabolites, or metabolome, over time or under different conditions generates a metabolite or metabolomic profiling. These changes occur through biochemical reactions, leading to the study of metabolic pathways. Tracking a mixture or set of metabolites is essential for providing a dynamic view of

metabolome, generating metabolomic profiles, studying metabolic pathways, and more.

**1D NMR Spectroscopy Tracking Metabolomes.** The identification and quantification of metabolites using 1D NMR techniques were introduced in a previous section. Comparative analysis of the spectra collected at various conditions from the same metabolomic sample allows the study of related parameters and reactions. Nieves Embade et al. reported their study on inherited errors of metabolism in 2019.<sup>49</sup> They screened urine samples from 470 newborns using 1D <sup>1</sup>H NMR, and by comparing the spectra, they tracked differences in the metabolome, particularly in concentrations. For instance, they observed that three metabolites—3OH-butyric acid, acetoacetic acid, and acetone—showed significantly higher concentration in one spectrum compared to others, which were within the normal range, which suggested ketosis of this particular individual (Figure 4).

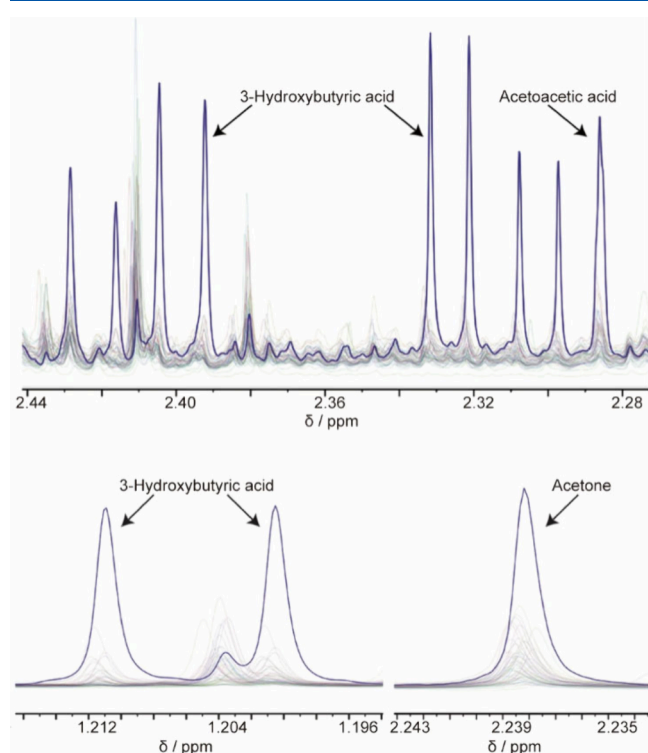


**Figure 4.** Stacked NMR spectra of the metabolome of the urine sample from the newborns, where iconic metabolites were identified, including 3OH-butyric acid, acetoacetic acid, and acetone. Reprinted by permission from Macmillan Publishers Ltd.: SCIENTIFIC REPORTS, Embade, N.; Cannet, C.; Diercks, T.; Gil-Redondo, R.; Bruzzone, C.; Ansó, S.; Echevarría, L. R.; Ayucar, M. M. M.; Collazos, L.; Lodoso, B.; Guerra, E.; Elorriaga, I. A.; Kortajarena, M. Á.; Legorburu, A. P.; Fang, F.; Astigarraga, I.; Schäfer, H.; Spraul, M.; Millet, O., NMR-based newborn urine screening for optimized detection of inherited errors of metabolism. *Sci. Rep.* 2019, 9 (1), 13067 (ref 49). Copyright 2019.

Arthur Edison and co-workers reported an extended application of high-resolution NMR for continuous *in vivo* monitoring of metabolism, along with accompanying analytical methods in 2019.<sup>50</sup> In part of this study, they prepared analyte samples by extracting a piece of *N. crassa* tissue after incubation in a nutrient-rich liquid medium for 32 h. They then continuously tracked the metabolome over 11 h using <sup>1</sup>H NMR spectra (Figure 5). After identification of the metabolites

and integration of the respective peaks, they plotted the variation trend of citrate, succinate, and glutamate over time.

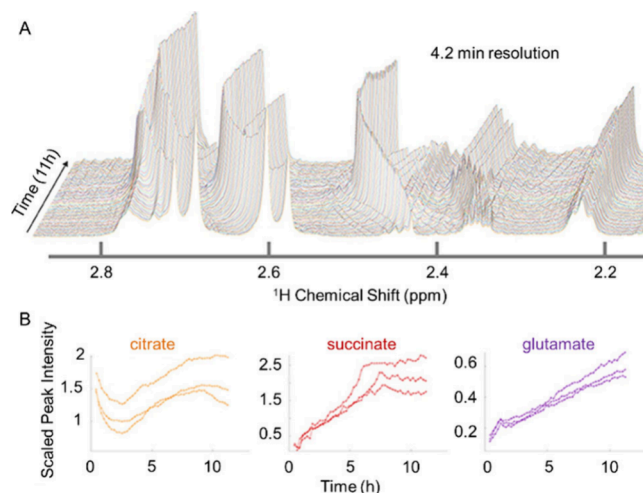


**Figure 5.** NMR experiment analysis of *N. crassa* tissue. A. processed and normalized high-resolution <sup>1</sup>H NMR spectra stacked; each collection was averaged over 64 scans at a resolution of 4.23 min. B. quantified and annotated trajectories of change of three metabolites: citrate, succinate, and glutamate. Reproduced from Judge, M. T.; Wu, Y.; Tayyari, F.; Hattori, A.; Glushka, J.; Ito, T.; Arnold, J.; Edison, A. S. Continuous *in vivo* metabolism by NMR. *Front. Mol. Biosci.* 2019, 6, 26 (ref 50). Copyright 2019 Frontiers.

Thore Buergel et al. reported their work on generating metabolomic profiles using NMR technique and computational power to predict the risk of 24 common diseases on individuals in 2022.<sup>51</sup> They analyzed 1D <sup>1</sup>H NMR spectra of blood samples to generate metabolomic profiles and established the correlations between metabolomic states and incident rates under 24 common conditions. They also summarized the performance of combining age, sex, and metabolomic state for predicting 10-year outcomes across 15 end points. Additionally, they trained a neural network on data from the UK Biobank to validate the models based on metabolomic states. NMR-derived metabolomic profiles can assist multidisease assay, though further developments are still needed.

**Low Field NMR.** NMR spectroscopy typically operates at magnetic field strengths corresponding to proton resonance frequencies between 300 MHz (7 T) and 1000 MHz (23.5 T), whereas low field NMR runs at much lower fields, often around 85 MHz (2 T) or below. Compared to regular or high field NMR, low field NMR is more cost-effective, portable, and maintenance-friendly, making it particularly suitable for clinical and industrial applications.

Benita Percival et al. reported their research on utilization of low field NMR for point-of-care diagnostics of metabolic conditions in 2019.<sup>52</sup> Their study validated the detection of specific biomolecules employing a 60 MHz low field NMR spectrometer, enabling the identification of common metabolites associated with diabetes in readily accessible biofluids. They also developed a comprehensive protocol to facilitate the utilization of low-field NMR in metabolomics applications.

Jeremy Nicholson and co-workers reported their work on measurement of metabolites related to COVID-19 and inflammatory using low field <sup>1</sup>H NMR spectroscopy in 2022.<sup>53</sup> They incorporated relaxation, diffusion, and J-

modulation peak editing techniques (also referred to as the JEDI NMR method) to overcome challenges such as reduced spectral dispersion and strong coupling effects typical of low field NMR, enabling quantitative measurements of metabolites in human serum. Their investigation of a SARS-CoV-2 positive cohort demonstrated that the detection and quantification of the key metabolites could be successfully reproduced on an 80 MHz spectrometer at 298 K, matching results obtained from high-field instruments (600 MHz) under comparable conditions.

Despite these advancements, low field NMR still faces limitations, primarily due to its lower spectral resolution and weaker signal sensitivity. These constraints result in reduced spectral information and reduced applicability for complex samples. To address these challenges, ongoing research focuses on methods to enhance the resolution, sensitivity, and overall performance of low field NMR, broadening its potential applications.

**Enhancing Accuracy in Tracking and Quantifying Specific Metabolites in the Set.** The metabolome consists of mixtures of metabolites that can have very similar chemical environments, often resulting in overlapping NMR signals. High-resolution NMR offers improved signal separation, allowing for more accurate distinction of individual metabolites and the accurate integration of peaks for quantification. It also provides well-defined peaks, enhancing the interpretation of structural information. Additionally, high-resolution NMR offers higher sensitivity to minor and rapidly changing metabolites, enabling the detection of low-abundance compounds and more precise tracking of dynamic metabolic changes. Commonly used high-resolution NMR techniques include high magnetic field strength, quantitative NMR (qNMR), magic-angle spinning (MAS) NMR, and isotopic labeling, among others.

**Quantitative NMR.** Quantitative NMR (qNMR) focuses on the accurate integration of peaks to quantify metabolites, particularly in complex mixtures. It is typically performed on solution samples to determine compound concentration or purity, often using an empirically derived “response factor” or an internal reference with a known concentration. qNMR experiments are usually conducted at magnetic field strengths of 500 MHz or higher. For accurate qNMR analysis, it is essential that the spectrum is well-phased and free from baseline distortions, as these factors obscure the determination of integrated signals and the selection of integral regions.

Obtaining accurate signal integrals can be particularly challenging where signals overlap or are very close or when the signal-to-noise ratio is limited. Fernando Violante et al. reported their research on the utilization and optimization of  $^1\text{H}$  and  $^{13}\text{C}$  qNMR for the purity analysis of nitrofur metabolites.<sup>54</sup> They evaluated the purity of 3-amino-2-oxazolidinone (AOZ), 3-amino-5-morpholinomethyl-2-oxazolidinone (AMTZ), and 1-aminohydantoin (AHD) using  $^1\text{H}$  qNMR and developed a more accurate  $^{13}\text{C}$  qNMR method. When compared with quantitative analysis via a mass balance approach and liquid chromatography, the optimized qNMR method demonstrated comparable and consistent results.

In our recent work, a concentration-ordered NMR spectroscopy (CORDY) was proposed for mixture analysis in 2021.<sup>55</sup> Based on the principle that the ratio of the NMR peak area to its corresponding number of spins is proportional to the concentration of the assigned compound, the CORDY method generated a pseudo-two-dimensional NMR spectrum,

enabling accurate quantification of metabolites in complex mixtures. The approach was validated with amino acids, soft drinks, and human urine samples. For the analysis of human urine, a chemical shift region ranging from 6.3 to 9.4 ppm was selected, and a CORDY plot was constructed, where the equivalent CH ( $N = 2$ ) was defined based on the ratio of the peak area, leveraging established chemical knowledge (Figure 6). Peaks corresponding to 10 molecules were identified and

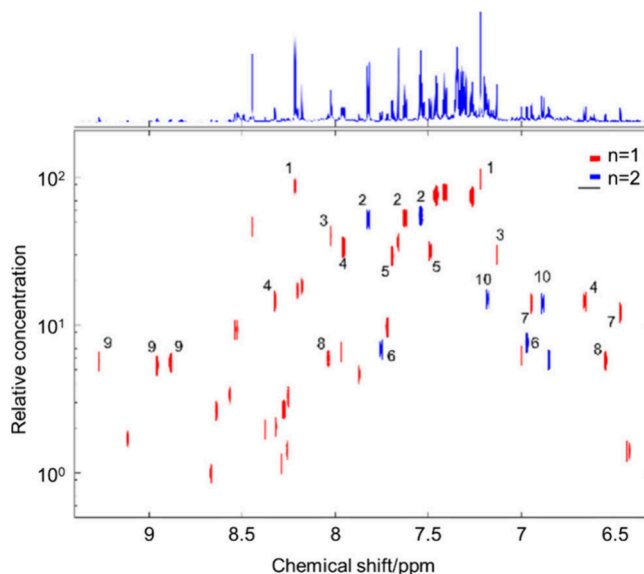


**Figure 6.**  $^1\text{H}$  CORDY plot of the human urine spectrum of the CH region ( $\delta$  6.3– $\delta$  9.4). Peaks from 10 molecules (labels 1 and 10) were identified. The line width along the concentration dimension was defined by  $\Delta$ . Reproduced from Yuan, B.; Zhou, Z.; Kamal, G. M.; Zhang, X.; Zhou, X.; Liu, M. NMR for mixture analysis: concentration-ordered spectroscopy. *Anal. Chem.* 2021, 93, 9697–9703 (ref 55). Copyright 2021 American Chemical Society.

labeled. Specifically, three peaks for hippurate were observed at 7.823, 7.624, and 7.641 ppm. The results demonstrated that CORDY is effective for analyzing mixtures with high dynamic content, spanning up to 2 orders of magnitude in concentration. Additionally, the combination of CORDY with DOSY methods further enhanced the resolution for molecules with similar concentrations or diffusion coefficients.

**High-Resolution MAS NMR.** Magic-angle spinning (MAS) NMR enhances the spectral resolution by rapidly spinning solid samples at a specific angle (usually  $54.74^\circ$ ) relative to the magnetic field. The spinning angle, known as the “magic angle”, effectively averages out anisotropic interactions, which are especially prominent in solid samples. By reducing these interactions, MAS NMR produced narrower peaks and clearer spectra, greatly improving the resolution for structural and quantitative analysis in solid-state studies.

In our previous work, a study examining metabolic changes in temporal lobe structures during the early stage of epilepsy was conducted with MAS NMR technique.<sup>56</sup> Metabolites in the bilateral hippocampi, entorhinal cortices (ECs), and temporal lobes (TLs) of rats were measured and analyzed, revealing significant metabolic profile differences between experimental and control (sham) groups in the bilateral hippocampi and ipsilateral EC (Figure 7). MAS NMR was specifically utilized to analyze metabolite with the HPC-EC loops, ensuring detailed observation of any metabolic changes.



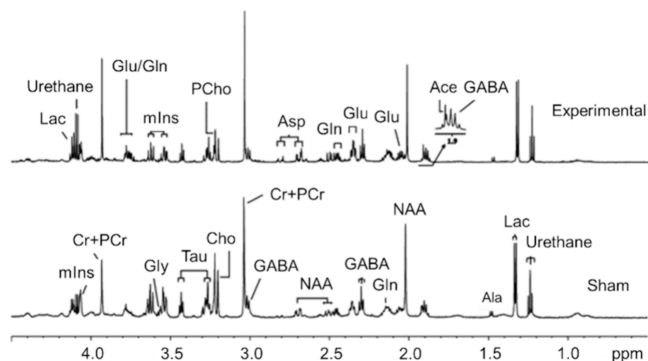


**Figure 7.** HR-MAS  $^1\text{H}$  NMR spectra of the metabolome in the rat brain; major metabolites were identified and labeled. The desired signals are sufficiently distinct for reliable quantification analysis. Reprinted from *Exp. Neurol.*, Vol. 212, Liu, H.; Fang, F.; Zhu, H.; Xia, S.; Han, D.; Hu, L.; Lei, H.; Liu, M. Metabolic changes in temporal lobe structures measured by HR-MAS NMR at early stage of electrogenic rat epilepsy, pp. 377–384 (ref 56). Copyright 2008, with permission from Elsevier.

These variations in metabolic profiles across brain regions provide insights into the distinct metabolic dynamics in temporal lobe structures, contributing to a better understanding of early state epileptic abnormalities.

**Isotopic Labeling.** Isotopic labeling increases the abundance of NMR-sensitive nuclei, particularly isotopes such as  $^{13}\text{C}$  or  $^{15}\text{N}$ , which have low natural abundance. By boosting the concentration of these nuclei, isotopic labeling enhances signal intensity and resolution, making it possible to obtain clearer and more detailed NMR signals.

Robin de Graaf et al. conducted research on kinetic isotope effects (KIE) using glucose and acetate in rat glioma cells and brain tissue.<sup>57</sup> Labeling the C3 position of lactate enhanced the signal-to-noise ratio of  $^{13}\text{C}$  NMR spectra, aiding in the tracking and quantification of lactate species derived from glucose substrates (Figure 8). In addition to deuterium-based isotopic labeling studies, they revealed KIEs for various metabolites, which contributed to the development of quantitative deuterium metabolic imaging techniques for mapping metabolic flux *in vivo*.

## METHODS FOR *IN SITU* AND *IN VIVO* STUDIES OF METABOLITES AND METABOLOMES

*In situ* NMR techniques here refer to the application of NMR spectroscopy to investigate metabolites within their native biological environments, such as in living cells or tissues, enabling real-time monitoring of metabolomes and metabolic processes. Given the complexity of cellular environments, these studies often require high-sensitivity and noninvasive NMR methods.

**In-Cell NMR.** Conventional metabolomics measures metabolite profiles at a steady state, typically at a single time point. In-cell NMR, however, enables the investigation of dynamic metabolic processes in living cells over time without needing cell extraction, thus, closely approximating physiological conditions. Although this approach faces technical challenges—such as low NMR sensitivity, reduced cell viability over long experiments, and signal broadening. Advances in sensitivity, resolution, and data acquisition speed have significantly improved metabolite identification and quantification in real time.

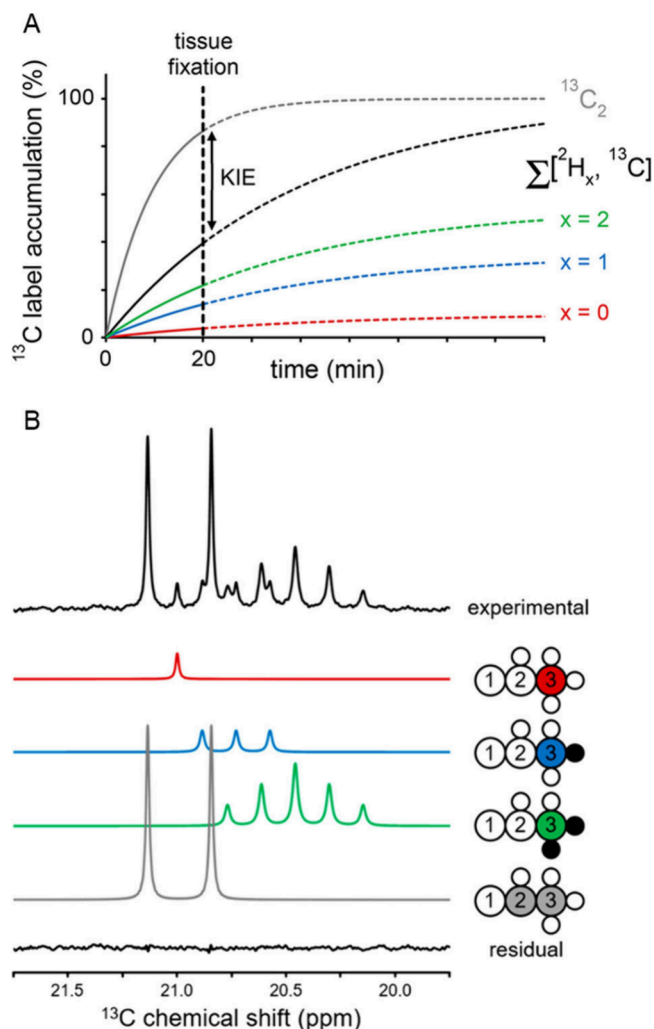


**Figure 8.** KIE study using  $^2\text{H}/^{13}\text{C}$  labeled lactates. A. Isotopic label accumulation curves for  $^{13}\text{C}$ -labeled lactate product in the presence of a significant KIE. B. 1D  $^{13}\text{C}$  NMR spectra showing different  $^{13}\text{C}$ -labeled lactate species. Reproduced from de Graaf, R. A.; Thomas, M. A.; Behar, K. L.; De Feyter, H. M. Characterization of kinetic isotope effects and label loss in deuterium-based isotopic labeling studies. *ACS Chem. Neurosci.* 2021, 12, 234–243. (ref 57). Copyright 2020 American Chemical Society.

The research discussed in section 3.1 on monitoring metabolism of *N. crassa* tissues employed in-cell NMR.<sup>50</sup> Another example is the work of Faezah Nami et al. reported in 2022, which used in-cell NMR to study fermentation and lipid metabolism processes in live microalgae cells.<sup>58</sup> They began by preparing live cell samples for an NMR study. By using  $^{13}\text{C}$  MAS NMR-based direct polarization (DP) single-pulse experiments, they monitored the processes of fermentation and lipid metabolism over time (Figure 9). Their observation revealed the conversion of galactolipids into triacylglycerol (TAG) and free fatty acids, accompanied by rapid loss of rigid lipid structures. They concluded that high cell densities, reacting in dark anoxia conditions, induced lipid catabolism, and cell death would lead to breakdown of cell and organelle membranes.

**In Vivo MRS.** *In vivo* magnetic resonance spectroscopy (MRS) is a noninvasive technique based on NMR principles, allowing for the detection of metabolites and their concentrations in living tissues.<sup>59,60</sup> Like NMR, MRS involves exciting

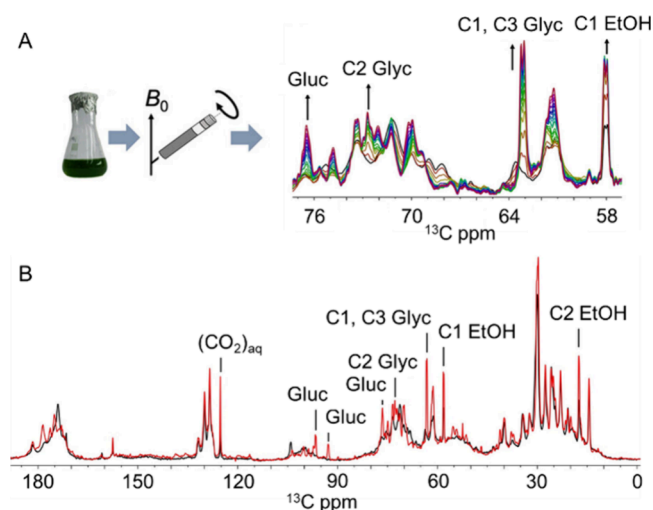


**Figure 9.**  $^{13}\text{C}$  MAS NMR of live microalgae cells, monitoring cellular processes, and structural dynamics changes. A. Demonstration of protocol of sample preparation and data acquisition where time-dependent series of  $^{13}\text{C}$  NMR spectra were collected. B.  $^{13}\text{C}$  NMR of the metabolome in cells after 1 h (black) and 24 h (red) of the process, signals of ethanol (EtOH), glycerol (Glyc), glucose (Gluc) and aqueous  $\text{CO}_2$  are identified and labeled. Reproduced from Real-time NMR recording of fermentation and lipid metabolism processes in live microalgae cells, F. Nami; Ferraz, M. J.; Bakkum, T.; Aerts, J. M. F. G.; Pandit, A. *Angew. Chem. Int. Ed. Engl.*, Vol. 61, Issue 14 (ref 58). Copyright 2022 Wiley.

nuclei within a specific volume using magnetic resonance and analyzing the resulting spectrum, which displays signal intensity versus frequency.<sup>61</sup> Compared to NMR, MRS can track metabolites of interest in selected regions within the living tissue and human body, and detect metabolic changes linked to the development and progression of diseases focused.<sup>62–64</sup> MRS is particularly valuable for clinical diagnostics, such as oncology and radiology,<sup>60,65,66</sup> and is often combined with magnetic resonance imaging (MRI) technique to provide both structural imaging and chemical composition insights. Frequencies in MRS equipment can target resonances of various nuclei (e.g.,  $^1\text{H}$ ,  $^{13}\text{C}$ ,  $^{31}\text{P}$ ), with  $^1\text{H}$  being most common due to its abundance and strong signal.<sup>67</sup> Unlike conventional NMR, MRS can monitor metabolic changes within targeted tissue regions, offering insights into disease progression.

Chaoyang Liu, and co-workers recently reported their research exploring metabolic aberrations after intracerebral hemorrhage (ICH) using *in vivo* MRS and MRI.<sup>68</sup> With the *in vivo*  $^2\text{H}$  MRS and MRI method, they demonstrated higher lactate concentration in ICH rats compared to the control group (Figure 10). Additionally, they detailed their advancements in MRS/MRI instrumentation and analytical methods, which improved the signal-to-noise ratio, thereby enhancing the feasibility of  $^2\text{H}$  MRS and MRI for *in vivo* metabolic studies and potential ICH assessment.

## RECENT PROGRESS OF THE APPLICATION OF NMR HYPERPOLARIZATION

The main factor limiting the broader application of NMR is its low sensitivity. The signal in NMR originates from the polarization of nuclear magnetic moments in a magnetic field, which is the difference in population between the Zeeman energy levels. Due to the very small gyromagnetic ratio of

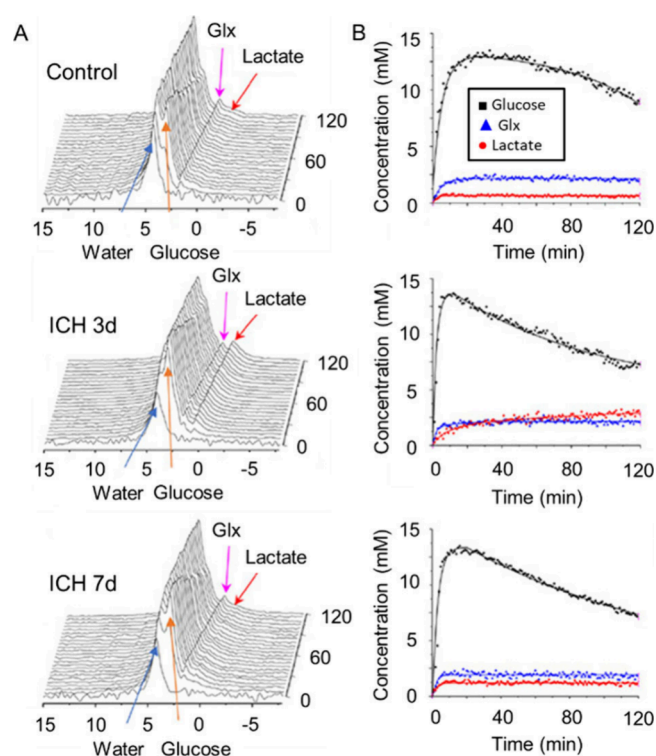


**Figure 10.** monitoring of changes of the metabolome using the *in vivo* MRS method. A. Over time with collection of  $^2\text{H}$  spectra of control, ICH 3d, and ICH 7d rats after  $[6,6'\text{-}^2\text{H}_2]$ -glucose injection, metabolites glutamate/glutamine (Glx) and lactate were identified and labeled. B. plots of metabolic dynamic curves of glucose, Glx, and lactate of control, ICH 3d and ICH 7d rats. Reproduced from Liu, X.; Bao, Q.; Liu, Z.; Wang, J.; Otikovs, M.; Zhang, Z.; Cheng, X.; Wang, J.; Frydman, L.; Zhou, X.; Liu, M.; Liu, C. Exploring metabolic aberrations after intracerebral hemorrhage *in vivo* with deuterium metabolic spectroscopy imaging. *Anal. Chem.* 2024, 96, 15563–15571 (ref 68). Copyright 2024 American Chemical Society.

atomic nuclei, the nuclear magnetic moments are very weak. This results in a small polarization of nuclear spins in the magnetic field, leading to the low sensitivity of NMR. Therefore, for a long time, improving NMR sensitivity has been one of the important goals pursued by the NMR community. In addition to conventional methods for enhancing NMR sensitivity, such as using magnets with a higher field strength and cryogenic probes, NMR sensitivity can also be significantly enhanced by increasing the polarization of nuclear spins in the sample. This type of methods is known as hyperpolarization.<sup>69</sup>

Common NMR hyperpolarization methods mainly include dynamic nuclear polarization (DNP),<sup>70</sup> chemically induced dynamic nuclear polarization (CIDNP),<sup>71</sup> parahydrogen-induced polarization (PHIP),<sup>72</sup> and signal amplification by reversible exchange (SABRE).<sup>73</sup> Recently, there have been significant advancements in the application of these methods in NMR analysis.

**DNP.** Due to the fact that the gyromagnetic ratio of electrons is approximately 660 times that of  $^1\text{H}$  nuclei, their polarization in a magnetic field is also much higher than that of nuclei. DNP technique significantly enhances NMR sensitivity by applying microwaves at an appropriate frequency to a sample containing unpaired electrons in a magnetic field, thereby transferring the high polarization of the electrons to the nuclei.<sup>70</sup> Although DNP can enhance the sensitivity of



liquid samples through the Overhauser effect, it is more commonly used for solid samples. For liquid samples, they can be frozen into solid samples, enhanced by DNP, and then dissolved before NMR or MRI experiments. This technique is known as dissolution DNP (dDNP).<sup>70</sup>

DNP transfers the polarization of unpaired electrons to the nuclei via microwave irradiation. Therefore, as providers of unpaired electrons, polarizing agents usually free radicals are a crucial component for the success of DNP experiments. The properties of free radicals, such as homogeneous line width ( $\delta$ ), the inhomogeneous breadth of their EPR spectrum ( $\Delta$ ), and g-anisotropy, significantly affect the effectiveness of DNP experiments. In addition to these properties, the polarization build-up time and quenching caused by the paramagnetism also affect the overall enhancement of NMR sensitivity. Venkatesh et al. utilized the overall sensitivity factor, a parameter that comprehensively considers the sensitivity enhancement factor, polarization build-up time, and quenching contributions, to compare the DNP enhancement performance of a series of nitroxide radicals under conditions of 9.4T and 100 K. They found that NaphPol and HydroPol exhibited the best sensitivity enhancement in organic solvents and aqueous solvents, respectively, while AMU-PolCbm performed well in both types of solvents.<sup>74</sup> Sakamoto et al. modified a pentacene molecule, a commonly used polarizing agent for triplet-DNP, enabling it to bypass the orientation requirements for samples, and acquire DNP sensitivity enhancement under milder experimental conditions.<sup>75</sup> Yau et al. proposed two new types of nitroxide-based triradicals, sulfoacetyl-DOTOPA and PEG12-DOTOPA, which have significantly faster polarization build-up times compared to common biradicals.<sup>76</sup>

After hyperpolarizing molecular probes using DNP, they can be applied to molecular imaging to detect certain chemical or biological processes. Currently, the most widely used molecular probe in *in vivo* dDNP hyperpolarized molecular imaging is  $[1-^{13}\text{C}]$  pyruvate, which has demonstrated great value in tumor research and metabolic imaging. As previously mentioned, triplet-DNP can achieve sample hyperpolarization under milder conditions. However, triplet-DNP relies on hydrophobic polarizing agents for the hyperpolarization of  $^{13}\text{C}$  nuclei, which poses challenges when applying triplet-DNP to hydrophilic  $[1-^{13}\text{C}]$  pyruvate. Hamachi et al. successfully achieved triplet-DNP hyperpolarization of  $^{13}\text{C}$  spins of sodium pyruvate by preparing a supramolecular complexation of a hydrophilic derivative of the commonly used triplet-DNP polarizing agent pentacene with beta-cyclodextrin.<sup>77</sup>

In addition to the aforementioned polarizing agent and polarizing target, the DNP experimental method is also continuously evolving. In conventional continuous-wave (CW) DNP experiments, the sensitivity enhancement factor decreases as the magnetic field strength increases. However, in pulsed DNP experiments, the sensitivity enhancement factor is independent of the magnetic field strength. Pulsed DNP technology also reduces the sample heating in microwave irradiation. Therefore, pulsed DNP technology has great application prospects in high-field DNP experiments. Redrout et al. proposed a new DNP pulse sequence.<sup>78</sup> This sequence is named XiX (X-inverse-X) DNP and consists of a series of repeated modules consisting of two pulses with opposite phases. Compared with previous DNP pulse sequences, XiX DNP requires lower microwave power and also achieves a higher sensitivity enhancement factor.

Applying dDNP to hyperpolarize  $[1-^{13}\text{C}]$ -pyruvate is of significant value in metabolic imaging and tumor research. The most common  $^{13}\text{C}$ -dDNP method involves using a narrow ESR line width radical, such as trityl, to transfer polarization directly from unpaired electron spins to  $^{13}\text{C}$  nuclei through microwave irradiation. This direct DNP method for electron- $^{13}\text{C}$  nuclei is time-consuming, typically taking about 1 h. Another method involves first polarizing  $^1\text{H}$  nuclei using a broad ESR line width radical, such as TEMPOL, and then transferring the polarization from  $^1\text{H}$  nuclei to  $^{13}\text{C}$  nuclei through cross-polarization (CP). This method is faster, typically taking about 20 min, but it requires high hardware and operator requirements. In addition to CP in the solid state, polarization can also be transferred from  $^1\text{H}$  nuclei to  $^{13}\text{C}$  nuclei through J-coupling in zero-field or ultralow-field conditions. This method has already been applied in parahydrogen-induced polarization (PHIP) experiments. Stern et al. proposed a technique called field inversion result in enhancement-dDNP (FIRE-dDNP).<sup>79</sup> This technique involves dissolving a sample that has already achieved  $^1\text{H}$  nuclear DNP enhancement and passing it through an adiabatic magnetic field inversion chamber. By  $^1\text{H}$ - $^{13}\text{C}$  J-coupling, the hyperpolarization is transferred from  $^1\text{H}$  nuclear spins to  $^{13}\text{C}$  nuclear spins. The authors demonstrated that using this technique, the  $^{13}\text{C}$  polarization in  $^{13}\text{C}$ -formate and  $[3-^{13}\text{C}]$ -pyruvate samples could be increased to 17% in just 10 min. This technique requires only minor modifications to the existing dDNP equipment.

$^1\text{H}$  NMR spectroscopy is an important analytical tool for metabolomics studies of biological fluid samples. However, severe signal overlap in the  $^1\text{H}$  NMR spectra is a significant limitation. Compared to  $^1\text{H}$  NMR,  $^{13}\text{C}$  NMR has a wider chemical shift range and narrower peak line widths, which can significantly alleviate peak overlap. Nevertheless, due to the low natural abundance and gyromagnetic ratio of  $^{13}\text{C}$  nuclei, using  $^{13}\text{C}$  NMR for NMR metabolomics analysis of biological fluids faces sensitivity challenges. Ribay et al. first reported the use of dDNP hyperpolarization to enhance the signal-to-noise ratio of  $^{13}\text{C}$  NMR spectra of natural abundance urine samples.<sup>80</sup> In dDNP experiments, various factors affect the peak intensity such as polarization efficiency and relaxation losses during the melting transfer process. Therefore, the study employed the standard addition method to obtain the absolute concentration of the analytes, and demonstrated that the  $^{13}\text{C}$  quantifiable concentration at natural abundance can be extended to approximately 1 mmol/L using dDNP hyperpolarization.

**CIDNP.** Some chemical reactions involving radical intermediates exhibit abnormally enhanced NMR signals of their products when they occur in a magnetic field. This phenomenon is known as chemically induced dynamic nuclear polarizations (CIDNP). Although the name includes DNP, its mechanism is different from DNP and actually originates from the radical pair mechanism.<sup>71</sup> Currently, CIDNP is often initiated by using photochemical reactions. Compared to DNP, CIDNP has a more limited range of hyperpolarization species but it can hyperpolarize solution samples at room temperature, which only requires laser irradiation of the sample, making it simpler in terms of instrument requirements.

CIDNP effect is very sensitive to radical intermediates, so CIDNP experimental results contain rich information about the intermediates and pathways of chemical reactions. Worner et al. took advantage of the ability of time-resolved photo-CIDNP to detect information on radical intermediates,

observing the presence of the 5-deazaflavin radical, indirectly confirming that 5-deazaflavin can undergo single-electron transfer reactions.<sup>81</sup> Prior to this, 5-deazaflavin was generally believed to be similar to nicotinamide, only able to act as a two-electron transfer agent.

NMR can detect interactions between targets and ligands; therefore, it is used for drug screening. However, due to the low sensitivity of NMR, it requires a larger sample volume and longer instrument time, making high-throughput drug screening difficult to achieve. Torres et al. used photo-CIDNP to enhance the polarization of ligand molecules, enabling high-throughput drug screening of low  $\mu\text{M}$  concentration ligands and low  $\mu\text{M}$  unlabeled proteins. Before that work, only about 30 molecules were reported to have photo-CIDNP activity, so the first step of that study was to select 917 molecules with different aromatic scaffolds and substitutions from EU-OPENSREEN (EOS), and test their photo-CIDNP activity through standard photo-CIDNP experiments. They found that 340 of these molecules exhibited photo-CIDNP activity; then, they constructed a small-molecule library containing 287 compounds for fragment-based photo-CIDNP NMR screenings. Furthermore, based on solubility and enhanced CIDNP sensitivity, 212 molecules were selected for single-scan photo-CIDNP NMR detection with and without the PIN1 protein. If a compound binds to the target protein, the relaxation decay of the compound will be faster, resulting in a noticeable difference in signal intensity between the spectra obtained with and without the target protein. The authors applied this new method, which took 11 h, and discovered 20 ligands that interacted with the target protein out of 212 molecules.

One problem faced by photo-CIDNP experiments is that the required photosensitizer can sometimes undergo degradation. Gomez et al. designed a microfluidic chip with a planar spiral microcoil in an untuned circuit.<sup>82</sup> This chip can irradiate the sample with a laser through optical fibers, achieving photo-CIDNP polarization enhancement. It can easily optimize the experimental parameters of photo-CIDNP, such as the ratio of target molecules to photosensitizers. This flow setup also avoids the problem of photosensitizer degradation. In addition, using the planar spiral microcoil integrated into the chip, 1D or 2D three-nuclei NMR experiments can also be conducted.

NMR is a powerful tool for analyzing biofluids such as urine and serum as it provides qualitative and quantitative information about the components of the sample. However, due to the presence of a large number of metabolites in biological fluids, the NMR spectra often suffer from severe peak overlap. Kuhn et al. successfully collected photo-CIDNP NMR spectra of unaltered human urine and serum samples.<sup>83</sup> Photo-CIDNP activity is primarily found in molecules with low ionization energies, such as aromatics, which can participate in the radical pair mechanism that produces the CIDNP effect; therefore, the main components in biofluids that exhibit photo-CIDNP activity are four amino acids: tyrosine, tryptophan, histidine, and methionine. As expected, the resonance peaks of these four amino acids were found in the photo-CIDNP NMR spectra of the urine. In addition, other signals were detected in the spectra, which were attributed to several metabolites that are highly clinically relevant with certain diseases.

**PHIP.** The spin quantum number of the  $^1\text{H}$  nucleus is  $1/2$ . According to the Pauli exclusion principle, the singlet spin state of an  $\text{H}_2$  molecule (parahydrogen) must be accompanied by a nuclear rotational wave function with an even rotational quantum number  $J$ . Since the energy level difference of the

rotational quantum numbers is much greater than that of the nuclear spin quantum numbers, the distribution of nuclear quantum states of  $\text{H}_2$  molecule is primarily determined by the rotational quantum numbers. Under low temperature conditions, the proportion of parahydrogen increases. Parahydrogen Induced Polarization (PHIP) is the technique where the high spin order of parahydrogen is used to increase the polarization of  $^1\text{H}$  nuclei through the hydrogenation reaction of parahydrogen with substrate.<sup>72</sup> PHIP has been used for structural analysis of complexes, studying reaction mechanisms involving hydrogen and the production of contrast agents used in MRI.

Pyruvic acid plays a crucial role in the glycolytic pathway associated with inflammation, neurodegenerative diseases, and cancer.  $[1-^{13}\text{C}]$  pyruvate and  $[2-^{13}\text{C}]$  pyruvate have been reported to be used in metabolic studies of pyruvate after hyperpolarization.<sup>84</sup> However, both  $[1-^{13}\text{C}]$  pyruvate and  $[2-^{13}\text{C}]$  pyruvate cannot fully reflect the metabolic pathways of pyruvate. Stevanato et al. utilized the parahydrogen-induced polarization side arm hydrogenation (PHIP-SAH) technique and the MINERVA pulse sequence to obtain  $[1,2-^{13}\text{C}]$  pyruvate, and monitored the enzymatic conversion of pyruvate to lactate in vitro and in-cell via different carbon sites.<sup>85</sup> Moreover, they also observed the nonenzymatic decarboxylation process of  $[1,2-^{13}\text{C}]$  pyruvate using  $^{13}\text{C}$  NMR, detecting products such as acetate, carbon dioxide, bicarbonate, and carbonate.

Biochemical processes are often stereoselectively biased, as seen in the predominance of amino acids involved in these processes. Recent interest in D-amino acids has significantly increased due to their abnormal levels being associated with certain diseases. Nevertheless, distinguishing and quantifying the enantiomers of amino acids can be time-consuming and cumbersome. Dreisewerd et al. proposed a method based on parahydrogen-induced hyperpolarization that allows for the differentiation of D- and L- $\alpha$ -amino acids at the submicromolar concentration level. They use an iridium–heterocyclic carbene catalyst to bind with  $\alpha$ -amino acids in a bidentate manner, while also binding with parahydrogen and a cosubstrate. Parahydrogen binds and dissociates from the complex in a reversible manner, thereby maintaining hyperpolarization continuously. When the cosubstrate is chiral, such as (S)-nicotine, the hydride NMR signals of D- and L- $\alpha$ -amino acids exhibit different chemical shifts. Utilizing this method, combined with the capability of two-dimensional zero-quantum experiments to alleviate spectral peak overlap, the authors differentiated the enantiomers in a racemic mixture of 16  $\alpha$ -amino acids. Additionally, they used the same method to detect D- $\alpha$ -amino acids in a methanolic extract of instant coffee.

As mentioned above, chirality plays a crucial role in living systems. In order to better utilize NMR techniques for studying chiral metabolites, there is a need to obtain chiral-selective hyperpolarized metabolites. Huynh et al. proposed the stereoPHIP technique, which is a novel approach for obtaining chiral-selective hyperpolarized metabolites.<sup>86</sup> StereoPHIP uses a chiral rhodium(I) catalyst for the catalytic addition of parahydrogen to the prochiral precursor O-acetyl ethyl enolpyruvate, under ALTADENA conditions, resulting in  $^1\text{H}$  hyperpolarized O-acetyl ethyl lactate. Subsequently, the hyperpolarization is transferred to the  $^{13}\text{C}$  nuclei through magnetic field cycling (MFC). They found that using the (R,R) type chiral catalyst yielded the L-product, while using the

(S,S) type chiral catalyst yielded the D-product. The chirality of the products was identified using chiral chromatography and high-resolution  $^1\text{H}$  NMR with a shift reagent.

**SABRE.** Signal Amplification by Reversible Exchange (SABRE) is a method within the PHIP (Parahydrogen Induced Polarization) techniques.<sup>73</sup> Traditional PHIP methods utilize parahydrogen to asymmetrically hydrogenate unsaturated substrates, thereby achieving hyperpolarization. Unlike traditional PHIP methods, SABRE employs a catalyst to form a reversible transient complex with parahydrogen and the substrate. After the substrate is hyperpolarized, it dissociates from the complex, becoming a free state of the hyperpolarized substrate. SABRE has at least two advantages: first, it does not require actual chemical modification of the substrate molecules; second, it allows for the continuous introduction of parahydrogen gas into the sample solution, maintaining a sustained hyperpolarized state of the substrate.

Due to their portability and low maintenance costs, benchtop NMR has increasingly gained attention in recent years. However, due to the low magnetic field strength of benchtop NMR spectrometers, their sensitivity is also low. Clearly, hyperpolarization techniques can significantly enhance the sensitivity of benchtop NMR. Kircher et al. have utilized the SABRE technique to achieve the  $^{15}\text{N}$  and  $^{13}\text{C}$  NMR measurement in natural isotopic abundant samples using benchtop NMR.<sup>87</sup> They proposed a spin-lock-induced cross-linking (SLIC) pulse sequence to transfer hyperpolarization from  $^1\text{H}$  nuclei to  $^{15}\text{N}$  or  $^{13}\text{C}$  nuclei within the catalyst-parahydrogen-substrate complex. After optimizing experimental parameters such as pulse frequency and amplitude, they achieved in situ SABRE hyperpolarization in a benchtop NMR spectrometer in just 10 s for ammonia, 4-aminopyridine, benzylamine, and phenethylamine dissolved in methanol or dichloromethane, with a  $^{15}\text{N}$  polarization of 12% and a  $^{13}\text{C}$  polarization of 0.4%.

Due to the low sensitivity of NMR, some components in biological fluids may be difficult to detect because their concentrations are below the NMR's limit of detection (LOD). The use of SABRE can significantly enhance the NMR detection sensitivity of biological fluids. However, due to the poor water solubility of the catalyst, it usually requires solid-phase extraction (SPE) of the sample followed by dissolution in methanol, which undoubtedly alters the state and composition of the sample. Ausmees et al. found that ammonia and urea are significant impediments to sample SABRE hyperpolarization and proposed a sample preparation protocol that avoids the SPE step, removes ammonia and urea, and achieves parahydrogen hyperpolarization of minimally altered urine samples.<sup>88</sup> The enhanced SABRE signal spectra detected are from the signals of the complexes formed by the substrates with the catalyst and parahydrogen, with chemical shifts in the range of  $-20$  to  $-24$  ppm, avoiding overlap with the spectral peaks of the free-state substrates. It should be noted that this method can detect only some components in biological fluids for metabolomics research.

When a ligand binds to a protein, multiple parameters of its NMR signal change; thus, NMR can be used to detect the interaction between ligands and proteins. However, the application of NMR-based screening of protein–ligand binding is still limited by the low sensitivity of NMR. The SABRE technique can be used to enhance the signal of ligands,<sup>89</sup> but it is impractical to perform SABRE hyperpolarization on all types of ligands. Mandal et al. proposed a very clever SABRE-based

screening of the protein–ligand binding method.<sup>90</sup> This method involves finding a ligand for the target protein called a reporter ligand that can be both hyperpolarized by SABRE and bind to the target protein. When the SABRE hyperpolarized reporter ligand is bound to the target protein, it will have a shorter transverse relaxation time compared to that of its free state. When other ligands in the sample interact with the target protein, they compete with the reporter for binding to the protein, causing changes in the transverse relaxation time of the reporter, typically a value between that of the free and bound states. By observing the transverse relaxation time of the reporter, screening of protein–ligand binding can be achieved, and it only requires the hyperpolarization of the reporter using SABRE. Later, Pham et al. extended this method to the study of biomolecular interactions using low-field NMR.<sup>91</sup>

## PERSPECTIVE

NMR spectroscopy has shown great applications in metabolic studies. The development and refinement of spectral simplification techniques, combined with the integration of computational methods and the generation of databases, will likely lead to more accurate and faster identification and quantification of metabolites. The extension of NMR applications to in-cell and *in vivo* environments provides a deeper understanding of metabolic processes in their natural contexts. Further advancements in these applications will depend on improvements in measurement sensitivity, signal resolution, and analytical accuracy. Enhancing established techniques such as MAS and isotopic labeling continues to offer substantial benefits, while the development of novel or integrated methodologies may also present valuable opportunities. Additionally, the continued exploration of low-field NMR holds promise for miniaturizing the instruments, thereby facilitating portable use and real-time metabolic monitoring, particularly in clinical or field settings. The reduction in the cost and maintenance requirements of NMR instrumentation could further broaden the accessibility and adoption of this technology. Furthermore, the application of hyperpolarization techniques enhances the sensitivity required for detecting low-abundance metabolites.

As these methods continue to develop, they are expected to provide valuable insights into metabolic pathways and contribute significantly to the field of metabolomics. Ongoing collaboration in optimizing NMR methods, mathematical analysis, and computational power will further unlock the potential of NMR spectroscopy in metabolite studies and metabolites analysis.

## AUTHOR INFORMATION

### Corresponding Author

**Maili Liu** – State Key Laboratory of Magnetic Resonance and Atomic Molecular Physics, National Center for Magnetic Resonance in Wuhan, Innovation Academy for Precision Measurement Science and Technology, Chinese Academy of Sciences, Wuhan 430071, China; University of Chinese Academy of Sciences, Beijing 101408, China; Optics Valley Laboratory, Hubei 430074, China; [orcid.org/0000-0002-9359-915X](https://orcid.org/0000-0002-9359-915X); Email: [ml.liu@wipm.ac.cn](mailto:ml.liu@wipm.ac.cn)

### Authors

**Lichun He** – State Key Laboratory of Magnetic Resonance and Atomic Molecular Physics, National Center for Magnetic



Resonance in Wuhan, Innovation Academy for Precision Measurement Science and Technology, Chinese Academy of Sciences, Wuhan 430071, China; University of Chinese Academy of Sciences, Beijing 101408, China; [orcid.org/0000-0002-0772-0452](https://orcid.org/0000-0002-0772-0452)

**Bin Jiang** — State Key Laboratory of Magnetic Resonance and Atomic Molecular Physics, National Center for Magnetic Resonance in Wuhan, Innovation Academy for Precision Measurement Science and Technology, Chinese Academy of Sciences, Wuhan 430071, China; University of Chinese Academy of Sciences, Beijing 101408, China

**Yun Peng** — State Key Laboratory of Magnetic Resonance and Atomic Molecular Physics, National Center for Magnetic Resonance in Wuhan, Innovation Academy for Precision Measurement Science and Technology, Chinese Academy of Sciences, Wuhan 430071, China; University of Chinese Academy of Sciences, Beijing 101408, China

**Xu Zhang** — State Key Laboratory of Magnetic Resonance and Atomic Molecular Physics, National Center for Magnetic Resonance in Wuhan, Innovation Academy for Precision Measurement Science and Technology, Chinese Academy of Sciences, Wuhan 430071, China; University of Chinese Academy of Sciences, Beijing 101408, China; [orcid.org/0000-0003-2481-946X](https://orcid.org/0000-0003-2481-946X)

Complete contact information is available at:

<https://pubs.acs.org/10.1021/acs.analchem.4c06477>

## Author Contributions

<sup>#</sup>L.H. and B.J. contributed equally to this work.

## Notes

The authors declare no competing financial interest.

## Biographies

Lichun He was awarded a Ph.D. fellowship from the Helmholtz Center for Infection Research in 2010 and received his Doctorate degree in 2014. Afterward, he worked together with Prof. Sebastian Hiller at University of Basel, Biozentrum, to investigate chaperone mechanisms. In 2019, he joined the Innovation Academy for Precision Measurement Science and Technology, CAS, China, with research interests in studies of biomolecular NMR spectroscopy.

Bin Jiang obtained his Ph.D degree in Radio Physics from Wuhan Institute of Physics and Mathematics, CAS. He is currently a Researcher at Innovation Academy for Precision Measurement Science and Technology, CAS. His research interest is mainly focused on NMR methodology.

Yun Peng obtained her Ph.D. degree in Chemistry from the University of Kansas in 2020. She is currently a Postdoctoral Fellow at the Innovation Academy for Precision Measurement Science and Technology, CAS, China, working on structure, function, and dynamics of metalloenzymes using solution NMR spectroscopy.

Xu Zhang obtained his Ph.D. degree in Radio Physics from Wuhan Institute of Physics and Mathematics in 2002. He is currently a Researcher at the Innovation Academy for Precision Measurement Science and Technology, CAS, China, with research interests in the development of NMR-based methods for the study of protein structure and dynamics.

Maili Liu is a Chief Scientist at the Innovation Academy for Precision Measurement Science and Technology, CAS. His research interests include development of novel NMR methodologies and applications for studying biomolecular structures and interactions.

## ACKNOWLEDGMENTS

This work is supported by the Strategic Priority Research Program of the Chinese Academy of Sciences XDB0540000, Natural Science Foundation of China grants 22327901, 22174151 and 21991080, and Hubei Provincial Natural Science Foundation of China 2023AFA041.

## REFERENCES

- (1) Inoki, K.; Zhu, T.; Guan, K.-L. *Cell* **2003**, *115* (5), 577–590.
- (2) Martínez-Reyes, I.; Chandel, N. S. *Nat. Commun.* **2020**, *11* (1), 102.
- (3) Krustrup, P.; Mohr, M.; Steensberg, A.; Bencke, J.; Kjær, M.; Bangsbo, J. *Medicine & Science in Sports & Exercise* **2006**, *38* (6), 1165.
- (4) Baker, S. A.; Rutter, J. *Nat. Rev. Mol. Cell Biol.* **2023**, *24* (5), 355–374.
- (5) Natarajan, N.; Florentin, J.; Johnny, E.; Xiao, H.; O'Neil, S. P.; Lei, L.; Shen, J.; Ohayon, L.; Johnson, A. R.; Rao, K.; Li, X.; Zhao, Y.; Zhang, Y.; Tavakoli, S.; Shiva, S.; Das, J.; Dutta, P. *Nat. Commun.* **2024**, *15* (1), 7337.
- (6) Song, Z.; Park, S. H.; Mu, W.-C.; Feng, Y.; Wang, C.-L.; Wang, Y.; Barthez, M.; Maruichi, A.; Guo, J.; Yang, F.; Lin, A. W.; Heydari, K.; Chini, C. C. S.; Chini, E. N.; Jang, C.; Chen, D. *Nature Aging* **2024**, *4*, 1384.
- (7) Zhu, J.; Thompson, C. B. *Nat. Rev. Mol. Cell Biol.* **2019**, *20* (7), 436–450.
- (8) Rathmell, J. C.; Fox, C. J.; Plas, D. R.; Hammerman, P. S.; Cinalli, R. M.; Thompson, C. B. *Mol. Cell. Biol.* **2003**, *23* (20), 7315–7328.
- (9) Esensten, J. H.; Helou, Y. A.; Chopra, G.; Weiss, A.; Bluestone, J. A. *Immunity* **2016**, *44* (5), 973–988.
- (10) Levitt, M. H. *J. Magn. Reson.* **2019**, *306*, 69–74.
- (11) Mamone, S.; Rezaei-Ghaleh, N.; Opazo, F.; Griesinger, C.; Glöggler, S. *Sci. Adv.* **2020**, *6* (8), No. eaaz1955.
- (12) Zangger, K. *Prog. Nucl. Magn. Reson. Spectrosc.* **2015**, *86–87*, 1–20.
- (13) Levitt, M. H. *Annu. Rev. Phys. Chem.* **2012**, *63* (1), 89–105.
- (14) Huang, C.; Peng, Y.; Lin, E.; Ni, Z.; Lin, X.; Zhan, H.; Huang, Y.; Chen, Z. *Anal. Chem.* **2022**, *94* (10), 4201–4208.
- (15) Xin, J. X.; Wei, D. X.; Ren, Y.; Wang, J. L.; Yang, G.; Zhang, H.; Li, J.; Fu, C.; Yao, Y. F. *Magn Reson Med.* **2023**, *89* (5), 1728–1740.
- (16) Lysak, D. H.; Kock, F. V. C.; Mamone, S.; Soong, R.; Glöggler, S.; Simpson, A. J. *Chem. Sci.* **2023**, *14* (6), 1413–1418.
- (17) Bax, A. *Journal of Magnetic Resonance (1969)* **1983**, *53* (3), 517–520.
- (18) Zangger, K.; Sterk, H. *J. Magn. Reson.* **1997**, *124*, 486–489.
- (19) Foroozandeh, M.; Adams, R. W.; Meharry, N. J.; Jeannerat, D.; Nilsson, M.; Morris, G. A. *Angew. Chem., Int. Ed. Engl.* **2014**, *53* (27), 6990–2.
- (20) Chen, X.; Caradeuc, C.; Montagne, A.; Baud, V.; Bertho, G.; Lucas-Torres, C.; Giraud, N. *Anal. Chem.* **2022**, *94* (43), 14974–14984.
- (21) Dal Poggetto, G.; Castañar, L.; Adams, R. W.; Morris, G. A.; Nilsson, M. *Chem. Commun. (Camb)* **2017**, *53* (54), 7461–7464.
- (22) Smith, M. J.; Castañar, L.; Adams, R. W.; Morris, G. A.; Nilsson, M. *Anal. Chem.* **2022**, *94* (37), 12757–12761.
- (23) Zhan, H.; Hao, M.; Lin, E.; Zheng, Z.; Huang, C.; Cai, S.; Cao, S.; Huang, Y.; Chen, Z. *Anal. Chem.* **2023**, *95* (2), 1002–1007.
- (24) Qiu, S.; Cai, Y.; Yao, H.; Lin, C.; Xie, Y.; Tang, S.; Zhang, A. Small molecule metabolites: discovery of biomarkers and therapeutic targets. *Signal Transduction and Targeted Therapy* **2023**, *8* (1). DOI: [10.1038/s41392-023-01399-3](https://doi.org/10.1038/s41392-023-01399-3)
- (25) Muthubharathi, B. C.; Gowripriya, T.; Balamurugan, K. *Molecular Omics* **2021**, *17* (2), 210–229.
- (26) Bezabeh, T.; Ijare, O. B.; Nikulin, A. E.; Somorjai, R. L.; Smith, I. C. *Magn Reson Insights* **2014**, *7*, 1–14.

- (27) Bezabeh, T.; Ijare, O. B.; Albiin, N.; Arnelo, U.; Lindberg, B.; Smith, I. C. P. *Magnetic Resonance Materials in Physics, Biology and Medicine* **2009**, 22 (5), 267–275.
- (28) Duarte, D.; Castro, B.; Pereira, J. L.; Marques, J. F.; Costa, A. L.; Gil, A. M. *Metabolites* **2020**, 10 (12), 515.
- (29) Kwan, E. E.; Huang, S. G. *Eur. J. Org. Chem.* **2008**, 2008 (16), 2671–2688.
- (30) Sims, E. K.; Carr, A. L. J.; Oram, R. A.; DiMeglio, L. A.; Evans-Molina, C. *Nature Medicine* **2021**, 27 (7), 1154–1164.
- (31) Hædersdal, S.; Andersen, A.; Knop, F. K.; Vilsbøll, T. *Nature Reviews Endocrinology* **2023**, 19 (6), 321–335.
- (32) Iftikhar, K.; Siddiq, A.; Baig, S. G.; Zehra, S. *Neuropeptides* **2020**, 79, No. 101993.
- (33) Piloizzi, A.; Carro, C.; Huang, X. *International Journal of Molecular Sciences* **2021**, 22 (1), 338.
- (34) Fu, J.; Zong, X.; Jin, M.; Min, J.; Wang, F.; Wang, Y. *Signal Transduction and Targeted Therapy* **2023**, 8 (1), 300.
- (35) Kościuczuk, E. M.; Lisowski, P.; Jarczak, J.; Strzałkowska, N.; Józwiak, A.; Horbańczuk, J.; Krzyżewski, J.; Zwierzchowski, L.; Bagnicka, E. *Molecular Biology Reports* **2012**, 39 (12), 10957–10970.
- (36) Roy, M.; Lee, R. W.; Brange, J.; Dunn, M. F. *J. Biol. Chem.* **1990**, 265 (10), 5448–5452.
- (37) Hua, Q. X.; Weiss, M. A. *Biochemistry* **1991**, 30 (22), 5505–15.
- (38) Wong, T. H. T.; Mo, J. M. Y.; Zhou, M.; Zhao, J. V.; Schooling, C. M.; He, B.; Luo, S.; Au Yeung, S. L. *Communications Biology* **2024**, 7 (1), 293.
- (39) Schleim, M. *AAPS Journal* **2017**, 19 (2), 397–408.
- (40) Gast, K.; Schüler, A.; Wolff, M.; Thalhammer, A.; Berchtold, H.; Nagel, N.; Lenherr, G.; Hauck, G.; Seckler, R. *Pharm. Res.* **2017**, 34 (11), 2270–2286.
- (41) Sitkowski, J.; Bocian, W.; Bednarek, E.; Urbaniak, M.; Koźmiński, W.; Borowicz, P.; Plucienniczak, G.; Łukasiewicz, N.; Sokółowska, I.; Kozerski, L. *Journal of Biomolecular NMR* **2018**, 71 (2), 101–114.
- (42) Caputo, N.; Castle, J. R.; Bergstrom, C. P.; Carroll, J. M.; Bakhtiani, P. A.; Jackson, M. A.; Roberts, C. T.; David, L. L.; Ward, W. K. *Peptides* **2013**, 45, 40–47.
- (43) Beaven, G. H.; Gratzner, W. B.; Davies, H. G. *Eur. J. Biochem.* **1969**, 11 (1), 37–42.
- (44) Gelenter, M. D.; Smith, K. J.; Liao, S.-Y.; Mandala, V. S.; Dregni, A. J.; Lamm, M. S.; Tian, Y.; Xu, W.; Pochan, D. J.; Tucker, T. J.; Su, Y.; Hong, M. *Nature Structural & Molecular Biology* **2019**, 26 (7), 592–598.
- (45) Wishart, D. S.; Guo, A.; Oler, E.; Wang, F.; Anjum, A.; Peters, H.; Dizon, R.; Sayeeda, Z.; Tian, S.; Lee, B. L.; Berjanskii, M.; Mah, R.; Yamamoto, M.; Jovel, J.; Torres-Calzada, C.; Hiebert-Giesbrecht, M.; Lui, V. W.; Varshavi, D.; Varshavi, D.; Allen, D.; Arndt, D.; Khetarpal, N.; Sivakumaran, A.; Harford, K.; Sanford, S.; Yee, K.; Cao, X.; Budinski, Z.; Liigand, J.; Zhang, L.; Zheng, J.; Mandal, R.; Karu, N.; Dambrova, M.; Schiöth, H. B.; Greiner, R.; Gautam, V. *Nucleic Acids Res.* **2022**, 50 (D1), D622–d631.
- (46) Huang, Z.; Chen, M. S.; Woroch, C. P.; Markland, T. E.; Kanan, M. W. *Chem. Sci.* **2021**, 12 (46), 15329–15338.
- (47) Garcia-Perez, I.; Posma, J. M.; Serrano-Contreras, J. I.; Boulangé, C. L.; Chan, Q.; Frost, G.; Stamler, J.; Elliott, P.; Lindon, J. C.; Holmes, E.; Nicholson, J. K. *Nat. Protoc.* **2020**, 15 (8), 2538–2567.
- (48) Xiao, X.; Wang, Q.; Zhang, X.; Jiang, B.; Liu, M. *Anal. Chem.* **2023**, 95 (45), 16567–16574.
- (49) Embade, N.; Cannet, C.; Diercks, T.; Gil-Redondo, R.; Bruzzzone, C.; Ansó, S.; Echevarría, L. R.; Ayucar, M. M. M.; Collazos, L.; Lodoso, B.; Guerra, E.; Elorriaga, I. A.; Kortajarena, M. A.; Legorburu, A. P.; Fang, F.; Astigarraga, I.; Schäfer, H.; Spraul, M.; Millet, O. *Sci. Rep.* **2019**, 9 (1), 13067.
- (50) Judge, M. T.; Wu, Y.; Tayyari, F.; Hattori, A.; Glushka, J.; Ito, T.; Arnold, J.; Edison, A. S. *Front. Mol. Biosci.* **2019**, 6, 26.
- (51) Buerger, T.; Steinfeldt, J.; Ruyoga, G.; Pietzner, M.; Bizzarri, D.; Vojinovic, D.; Upmeyer zu Belzen, J.; Looock, L.; Kittner, P.; Christmann, L.; Hollmann, N.; Strangalies, H.; Braunger, J. M.; Wild, B.; Chiesa, S. T.; Spranger, J.; Klostermann, F.; van den Akker, E. B.; Trompet, S.; Mooijaart, S. P.; Sattar, N.; Jukema, J. W.; Lavrijsen, B.; Kavousi, M.; Ghanbari, M.; Ikram, M. A.; Slagboom, E.; Kivimäki, M.; Langenberg, C.; Deanfield, J.; Eils, R.; Landmesser, U. *Nature Medicine* **2022**, 28 (11), 2309–2320.
- (52) Percival, B. C.; Grootveld, M.; Gibson, M.; Osman, Y.; Molinari, M.; Jafari, F.; Sahota, T.; Martin, M.; Casanova, F.; Mather, M. L.; Edgar, M.; Masania, J.; Wilson, P. B. *Protocols and Computational Models*. **2019**, 8 (1), 2.
- (53) Nitschke, P.; Lodge, S.; Hall, D.; Schaefer, H.; Spraul, M.; Embade, N.; Millet, O.; Holmes, E.; Wist, J.; Nicholson, J. K. *Analyst* **2022**, 147 (19), 4213–4221.
- (54) Bernstein, M. A.; Sýkora, S.; Peng, C.; Barba, A.; Cobas, C. *Anal. Chem.* **2013**, 85 (12), 5778–86.
- (55) Yuan, B.; Zhou, Z.; Jiang, B.; Kamal, G. M.; Zhang, X.; Li, C.; Zhou, X.; Liu, M. *Anal. Chem.* **2021**, 93 (28), 9697–9703.
- (56) Liu, H.; Fang, F.; Zhu, H.; Xia, S. A.; Han, D.; Hu, L.; Lei, H.; Liu, M. *Exp. Neurol.* **2008**, 212 (2), 377–85.
- (57) de Graaf, R. A.; Thomas, M. A.; Behar, K. L.; De Feyter, H. M. *ACS Chem. Neurosci.* **2021**, 12 (1), 234–243.
- (58) Nami, F.; Ferraz, M. J.; Bakkum, T.; Aerts, J.; Pandit, A. *Angew. Chem., Int. Ed. Engl.* **2022**, 61 (14), No. e202117521.
- (59) McLean, M. A.; Cross, J. J. *Br. J. Neurosurg.* **2009**, 23 (1), 5–13.
- (60) Tran, T.; Ross, B.; Lin, A. *Neurol. Clin.* **2009**, 27 (1), 21–60. xiii
- (61) Jansen, J. F.; Backes, W. H.; Nicolay, K.; Kooi, M. E. *Radiology* **2006**, 240 (2), 318–32.
- (62) An, L.; Shen, J. *Sci. Rep.* **2023**, 13 (1), No. 12211.
- (63) Penet, M. F.; Shah, T.; Wildes, F.; Krishnamachary, B.; Bharti, S. K.; Pacheco-Torres, J.; Artemov, D.; Bhujwalla, Z. M. *NMR Biomed* **2019**, 32 (10), No. e4053.
- (64) Castelli, D. D.; Terreno, E.; Longo, D.; Aime, S. *NMR Biomed* **2013**, 26 (7), 839–49.
- (65) Drost, D. J.; Riddle, W. R.; Clarke, G. D. *Med. Phys.* **2002**, 29 (9), 2177–97.
- (66) Gholizadeh, N.; Pundavela, J.; Nagarajan, R.; Dona, A.; Quadrelli, S.; Biswas, T.; Greer, P. B.; Ramadan, S. *Urol. Oncol.* **2020**, 38 (4), 150–173.
- (67) Harris, R. K.; Becker, E. D.; Cabral de Menezes, S. M.; Goodfellow, R.; Granger, P. *Solid State Nucl. Magn. Reson.* **2002**, 22 (4), 458–483.
- (68) Liu, X.; Bao, Q.; Liu, Z.; Wang, J.; Otikovs, M.; Zhang, Z.; Cheng, X.; Wang, J.; Frydman, L.; Zhou, X.; Liu, M.; Liu, C. *Anal. Chem.* **2024**, 96 (39), 15563–15571.
- (69) Kovtunov, K. V.; Pokochueva, E. V.; Salnikov, O. G.; Cousin, S. F.; Kurzbach, D.; Vuichoud, B.; Jannin, S.; Chekmenev, E. Y.; Goodson, B. M.; Barskiy, D. A.; Koptuyug, I. V. *Chem. Asian J.* **2018**, 13, 1857.
- (70) Michaelis, V. K. (Editor), Björn Corzilius, R. G. G. E. (Editor), Shimon, V. (Editor) *Handbook of High Field Dynamic Nuclear Polarization*. 2020.
- (71) Goetz, M., Chapter 3 Photo-CIDNP Spectroscopy. In *Annual Reports on NMR Spectroscopy*; Academic Press: 2009; Vol. 66, pp 77–147.
- (72) Duckett, S. B.; Mewis, R. E. Improving NMR and MRI Sensitivity with Parahydrogen. In *Hyperpolarization Methods in NMR Spectroscopy*; Kuhn, L. T., Ed.; Springer Berlin Heidelberg: Berlin, Heidelberg, 2013; pp 75–103.
- (73) Barskiy, D. A.; Knecht, S.; Yurkovskaya, A. V.; Ivanov, K. L. *Prog. Nucl. Magn. Reson. Spectrosc.* **2019**, 114–115, 33–70.
- (74) Venkatesh, A.; Casano, G.; Wei, R.; Rao, Y.; Lingua, H.; Karoui, H.; Yulikov, M.; Ouari, O.; Emsley, L. *Angew. Chem., Int. Ed. Engl.* **2024**, 63 (9), No. e202317337.
- (75) Sakamoto, K.; Hamachi, T.; Miyokawa, K.; Tateishi, K.; Uesaka, T.; Kurashige, Y.; Yanai, N. *Proc. Natl. Acad. Sci. U. S. A.* **2023**, 120 (44), No. e2307926120.
- (76) Yau, W. M.; Blake Wilson, C.; Jeon, J.; Tycko, R. *J. Magn. Reson.* **2022**, 342, No. 107284.

- (77) Hamachi, T.; Nishimura, K.; Sakamoto, K.; Kawashima, Y.; Kouno, H.; Sato, S.; Watanabe, G.; Tateishi, K.; Uesaka, T.; Yanai, N. *Chem. Sci.* **2023**, *14* (47), 13842–13850.
- (78) Redrouth, V. S.; Mathies, G. *J. Am. Chem. Soc.* **2022**, *144* (4), 1513–1516.
- (79) Stern, Q.; Reynard-Feytis, Q.; Elliott, S. J.; Ceillier, M.; Cala, O.; Ivanov, K.; Jannin, S. *J. Am. Chem. Soc.* **2023**, *145* (50), 27576–27586.
- (80) Ribay, V.; Dey, A.; Charrier, B.; Praud, C.; Mandral, J.; Dumez, J. N.; Letertre, M. P. M.; Giraudeau, P. *Angew. Chem., Int. Ed. Engl.* **2023**, *62* (27), No. e202302110.
- (81) Wörner, J.; Panter, S.; Illarionov, B.; Bacher, A.; Fischer, M.; Weber, S. *Angew. Chem., Int. Ed. Engl.* **2023**, *62* (43), No. e202309334.
- (82) Gomez, M. V.; Baas, S.; Velders, A. H. *Nat. Commun.* **2023**, *14* (1), 3885.
- (83) Kuhn, L. T.; Weber, S.; Bargon, J.; Parella, T.; Pérez-Trujillo, M. *Anal. Chem.* **2024**, *96* (1), 102–109.
- (84) Hu, S.; Yoshihara, H. A.; Bok, R.; Zhou, J.; Zhu, M.; Kurhanewicz, J.; Vigneron, D. B. *Magn Reson Imaging* **2012**, *30* (10), 1367–72.
- (85) Stevanato, G.; Ding, Y.; Mamone, S.; Jagtap, A. P.; Korchak, S.; Glöggler, S. *J. Am. Chem. Soc.* **2023**, *145* (10), 5864–5871.
- (86) Huynh, M. T.; Buchanan, E.; Chirayil, S.; Adebesein, A. M.; Kovacs, Z. *Angew. Chem., Int. Ed. Engl.* **2023**, *62* (46), No. e202311669.
- (87) Kircher, R.; Xu, J.; Barskiy, D. A. *J. Am. Chem. Soc.* **2024**, *146* (1), 514–520.
- (88) Ausmees, K.; Reimets, N.; Reile, I. *Chem. Commun. (Camb)* **2022**, *58* (3), 463–466.
- (89) Mandal, R.; Pham, P.; Hilty, C. *Chem. Sci.* **2021**, *12* (39), 12950–12958.
- (90) Mandal, R.; Pham, P.; Hilty, C. *Anal. Chem.* **2022**, *94* (32), 11375–11381.
- (91) Pham, P.; Hilty, C. *Chem. Sci.* **2023**, *14* (37), 10258–10263.